Published in "Food Hydrocolloids 25(7): 1766-1774, 2011"
which should be cited to refer to this work.

Structure of β-lactoglobulin microgels formed during heating as revealed by small-angle X-ray scattering and light scattering

Christian Moitzi [a], Laurence Donato [b], Christophe Schmitt [b], Lionel Bovetto [b], Graeme Gillies [a], Anna Stradner [a,*]

[a] Adolphe Merkle Institute, University of Fribourg, Rte de l'Ancienne Papeterie, P.O. Box 209, 1723 Marly 1, Switzerland
[b] Nestlé Research Center, Department of Food Science and Technology, PO Box 44, 1000 Lausanne 26, Switzerland

We have investigated the structure of microgels formed during heating of demineralized β-lactoglobulin (βlg) solutions at pH 5.9 by small-angle X-ray scattering (SAXS) and light scattering. First, unheated βlg solutions were characterized at different pH values between 2.0 and 7.0. At pH 5.9, βlg solutions contain mainly dimers (with a radius of approx. 2 nm), which coexist with a small number of larger oligomers (approx. 4 nm). Afterwards, βlg microgels, which form upon heating, were studied. They exhibit an average hydrodynamic radius around 130 ± 20 nm and an average molar mass around 7×10^8 g mol^{-1}. We followed the temporal evolution of the various structures that form after different heating times using subsequent SAXS measurements of the entire sample, the soluble fraction where the βlg microgels were removed, and the solvent. After an hour of heating at 85 °C the maximum yield of the βlg microgels (ca. 70%) is almost reached. Interestingly, the SAXS data show a correlation peak corresponding to a characteristic distance of about 9 nm, indicating an internal organization of the microgels. During the heating procedure the pH increases from pH 5.9 to approximately 6.6, which is induced by the partial conversion of βlg into βlg microgels that exhibit less buffering capacity than native protein. The remaining soluble fraction consists of native βlg and some small aggregates, whose number increases on the cost of native βlg as heating time proceeds. We propose that the formation of these lower molecular mass aggregates is triggered by the increased pH.

1. Introduction

Bovine whey proteins are widely used in food formulation because of their nutritional and functional properties (de Wit, 1998). β-lactoglobulin (βlg) accounts for approximately one half of the total mass of whey proteins (Morr & Ha, 1993). Heat treatment is often used during processing of food products for preservation purposes. This heat treatment may alter the structure, solubility and the functional properties of βlg (de Wit, 1998; Morr & Ha, 1993).

Previously βlg was described as a globular protein with a molar mass of approximately 18,400 g mol^{-1} and an isoelectric point at about pH 4.6 for the monomeric and pH 5.2 for the dimeric form (Hambling, McAlpine, & Sawyer, 1992; McKenzie, 1971). βlg exhibits different oligomerisation states, depending on the pH and the ionic strength (Timasheff, Mescanti, Basch, & Townend, 1966). Upon heating above its denaturation temperature (approx. 60 °C between pH 2 and pH 13) (Casal, Kohler, & Mantsch, 1988), βlg unfolds and forms aggregates through hydrophobic, electrostatic, and covalent chemical bonds (Bryant & McClements, 1998; Mulvihill & Donovan, 1987). The structure of these aggregates depends on the pH (Donald, 2008). Fibrils are formed at pH 2.0 (Aymard, Nicolai, Durand, & Clark, 1999; Kavanagh, Clark, & Ross-Murphyand, 2000), spherical particulates at pH 5.2 (Bromley, Krebs, & Donald, 2006) and fractal aggregates at pH 7.0 (Gimel, Durand, & Nicolai, 1994). Stable, non-sedimenting aggregates of βlg called βlg microgels (Mβlg), are formed upon heating a 1 wt% βlg solution in a narrow pH window and at low ionic strength (Schmitt et al., 2009). The specific pH regimes of 4.5 ± 0.1 and 5.9 ± 0.1 leading to the formation of Mβlg are close to the pH values of structural transitions which were previously reported (pH 4.0 and pH 6.0) (Langton & Hermansson, 1992). At these pH values the so-called fine-stranded and particulate βlg gels are formed at protein concentrations of 10 wt%. Mβlg were described as almost spherical aggregates with an average hydrodynamic radius

* Corresponding author. Tel.: +41 26 300 91 20; fax: +41 26 300 96 24.
E-mail address: anna.stradner@unifr.ch (A. Stradner).

between 100 and 200 nm and a polydispersity index below 0.2 (Donato, Schmitt, Bovetto, & Rouvet, 2009). Schmitt et al. (2009) reported that Mβlg formation results from an equilibrium of attractive hydrophobic forces, arising from the thermal protein denaturation, and repulsive electrostatic forces due to charges at these pH conditions. Recently, Donato et al. (2009) investigated the formation of Mβlg in a 1 wt% protein solution at pH 5.9 with different holding times at 70 °C and 85 °C. It was shown that at 70 °C activated βlg monomers form intermediate oligomers that aggregate to form Mβlg with hydrodynamic radii between 50 and 100 nm. After extended heating times only small non-sedimenting aggregates with hydrodynamic radii below 50 nm could be found. In contrast, Mβlg formation at 85 °C is faster and a reduced formation of intermediate oligomers is observed. The proposed explanation is that at 70 °C the slower aggregation rate leads to a larger pH shift during heating. The slower aggregation favors the formation of intermediate oligomers and soluble aggregates due to increased electrostatic repulsion.

Previous studies report structural features measured on the entire heated βlg system, irrespective of the relative composition with respect to the different aggregate species (Jung, Savin, Pouzot, Schmitt, & Mezzenga, 2008; Mehalebi, Nicolai, & Durand, 2008).

In this article the composition of βlg solutions under various heat treatment and pH conditions with respect to the different species formed as well as the structure of the resulting protein aggregates are revealed by 3D-cross-correlation dynamic light scattering and small-angle X-ray scattering (SAXS). Native samples are characterized at pH values between 2.0 and 7.0 while the effect of heat treatment is investigated on samples with a starting pH of 5.9. By using centrifugation steps we were able to separate the scattering signals of the Mβlg and non-Mβlg fraction (composed of residual native βlg and small non-sedimenting aggregates). Samples were taken during the heating from 20 to 85 °C, and during a holding period of up to 8 h at 85 °C.

2. Materials and methods

2.1. Demineralization of the raw material

β-Lactoglobulin (lot JE 003-6-922, 23/05/2006) was purchased from Davisco Foods International Inc. (Le Sueur, MN, USA). The powder contains 90.3 wt% protein (Kjeldahl analysis: N × 6.38). The major protein constituents are 54 wt% βlg variant A, 43 wt% βlg variant B, 2 wt% α-lactalbumin, and 1 wt% bovine serum albumin (BSA) as determined by hydrophobic interaction chromatography. The powder further contains 5 wt% water, 0.3 wt% fat, <1 wt% lactose and 1.8 wt% ash including 0.02 wt% Ca^{2+}, 0.009 wt% K^{+}, 0.02 wt% Mg^{2+}, 0.65 wt% Na^{+} and 0.051 wt% P (determined by HNO_3/H_2O_2 mineralization of the protein sample and analysis using a Vista MPX simultaneous ICP-AES spectrometer (Varian Inc. Palo Alto, CA, USA)).

A protein solution (500 mL) was prepared by dispersing 10 wt% βlg (protein content) in degassed MilliQ water (resistivity: 18.2 MΩ cm), and stirring for 1 h at 20 °C. The solution was then gently stirred at 4 °C for 12 h to allow complete hydration.

Demineralization of the sample was performed as follows. First, the denatured protein was precipitated by adjusting the pH to 4.6. The solution was then centrifuged at 25,600 g (Sorvall Instrument, rotor SLA-1000) for 15 min, the supernatant containing the native protein was collected and the pH was adjusted to 2.0. The protein solution was then filtered through 0.22 μm sterile microfilters (Stericup, Millipore), divided into four fractions and further purified by membrane dialysis (molecular weight cut-off of 6000–8000 Da, Spectra/Por, Spectrum laboratories, USA). The first dialysis step was against water at pH 2.0 and lasted 6 h. Afterwards the sample was dialyzed against 6 consecutive 20 L water baths at pH 6.0 and 4 °C. The demineralized βlg solution was then freeze dried and stored in desiccators until use.

A sample volume of 1 L of protein solution at 1 wt% was prepared by dispersing the demineralized βlg powder in degassed MilliQ water and stirred for 1 h at 20 °C. The protein dispersion was then gently stirred at 4 °C for 12 h. This procedure resulted in a turbid solution at pH 4.6 where the turbidity stems from the presence of insoluble material. After adjusting the pH to 7.0 with NaOH (1 M, Merck, Darmstadt, Germany) the solution became transparent and colorless. The solution of demineralized βlg was then filtered through 0.22 μm sterile microfilters (Stericup, Millipore). The mineral content of the sample determined by atomic adsorption spectroscopy was 0.00013 wt% Ca^{2+}, traces of K^{+}, 0.000065 wt% Mg^{2+}, 0.000067 wt% Na^{+}, and 0.05 wt% P. The protein concentration was checked by UV/Vis spectroscopy ($\epsilon_{280} = 0.953$ g dL cm^{-1} for the demineralized freeze dried powder as determined experimentally; Uvikon 810, Kontron Instruments, Flowspec, Switzerland).

2.2. Sample preparation and heat treatment

The demineralized βlg solution was adjusted from pH 7.0 to pH 6.2, 5.9, 5.6, and pH 2.0 with HCl (0.1 M Merck, Darmstadt, Germany), filtered through 0.22 μm membranes (hydrophilic Millex-GV PVDF syringe filters from Millipore) and characterized by DLS and SAXS immediately after pH adjustment.

The heat treatment was then performed on the solution adjusted to pH 5.9 as Mβlg form at this pH (Donato et al., 2009). Multiple samples consisting of 20 mL of protein solution in 20 mL glass vials with hermetically sealed rubber caps were heated simultaneously in a water bath at 85 °C for up to 8 h. The samples were stirred during heating. The temperature of the samples was assumed from the value of one sample vial equipped with a digital thermometer (Hanna, Hi 147-00). Samples were removed from the water bath when the temperature reached 60, 70, 75, 80 and 85 °C respectively. Three additional samples were left in the water bath for another period of 15, 60 and 480 min. Once removed from the heating bath, samples were placed in ice to quench the heat treatment. After recording the pH values the samples were stored at 4 °C.

2.3. Composition of the systems

The composition of the systems was determined with respect to the so-called "soluble fraction" (consisting of the small aggregates that do not sediment under the conditions applied in our centrifugation procedure described below, as well as of residual native βlg) and "insoluble fraction" (i.e. the larger aggregates called Mβlg, which do sediment when centrifuged according to our centrifugation protocol) (Donato et al., 2009).

The concentration of residual native protein in each sample was quantified by absorbance measurements at 280 nm after removing all denatured, aggregated protein. This was done by adding an acetic acid/sodium acetate buffer (0.5 M, pH 4.6) which precipitates all but the native protein. Samples were then centrifuged in Eppendorf tubes for 15 min at 16,870 g (Eppendorf centrifuge, rotor FA 451811). The concentration of the supernatant ($SN_{pH4.6}$) containing the residual native protein was determined.

The concentration of the "insoluble fraction" (Mβlg) was determined after centrifugation of the heated samples for 30 min at 16,870 g (Eppendorf centrifuge, rotor FA 451811), which leads to sedimentation of the βlg microgels. The absorbance of the supernatants (SN), which now contain the "total soluble fraction", was measured at 280 nm by spectrophotometry. The concentration of

the "insoluble fraction" was calculated from the difference between the absorbance of SN and the absorbance of the native sample.

The fraction of "soluble aggregates" was calculated by subtracting the residual native protein concentration from the "total soluble fraction".

Small-angle X-ray scattering and dynamic light scattering were used to determine the structure of the soluble and insoluble fraction by measuring the unfractionated heated samples as well as their corresponding supernatants (SN) containing the soluble fraction only.

2.4. Small-angle X-ray scattering

The small-angle X-ray scattering (SAXS) experiments were partially done at the Swiss Light Source (Paul Scherrer Institute, Switzerland) at the cSAXS instrument. At least fifty 2D images were taken at different positions of the sample to avoid radiation damage. The 2D images were radially integrated into the one-dimensional scattering function $I(q)$. The length of the scattering vector is defined as $q = (4\pi/\lambda)\sin(\Theta/2)$, where λ is the wavelength, and Θ is the scattering angle. Silver behenate was used to calibrate the q-scale. Averaging and background subtraction was done according to established procedures of the Paul Scherrer Institute.

Selected samples were measured with a SAXSess lab instrument (Anton Paar, Graz, Austria) (Bergmann, Orthaber, Scherf, & Glatter, 2000) which comprises an X-ray generator (PANalytical, PW 3830) with a sealed copper tube. The tube was operated at 50 mA and 50 kV. A Göbel mirror and a Kratky block collimation system were used to convert the divergent polychromatic X-ray beam into a focused line shaped beam of Cu-K_α radiation with a length of approx. 3 cm. The sample was filled into a quartz capillary of 1 mm diameter and 0.01 mm wall thickness. The capillary was placed along the line shaped X-ray beam in the evacuated camera housing. The 2D scattering pattern was recorded by an imaging plate detector (Packard Cyclone Storage Phosphor Screen with OptiQuant software) and integrated into the one-dimensional scattering function using the SAXSquant software (Anton Paar).

The absolute calibration was established from the scattered intensity of water, which depends on the isothermal compressibility and on the electron density only ($I(0)_{\text{water},25^\circ\text{C}} = 0.01633\ \text{cm}^{-1}$) (Orthaber, Bergmann, & Glatter, 2000).

The determination of the radius of gyration R_G was complicated by the fact that the samples were polydisperse and the scattering curves showed an upturn at small scattering vectors. The indirect Fourier transformation (IFT) (Glatter, 1977) method was used in order to obtain the radius of gyration R_G (Guinier & Fournet, 1955) and the extrapolation of the scattering intensity to an angle of zero $I(0)$ of the main protein fraction. The scattering curves, which were smeared due to the line shaped direct beam, were desmeared by the IFT algorithm.

The aggregation number of aggregates can be determined from SAXS data, as the forward scattering intensity at zero scattering angle $I(0)$ depends linearly on the molecular weight of the scattering particles. The molar mass of non-interacting aggregates can be calculated from Eq. (1) (Kratky, Porod, & Kahovec, 1951; Lindner & Zemb, 2002).

$$M = \frac{\mathrm{d}\Sigma(0)}{\mathrm{d}\Omega}\left(N_A/c\Delta\rho_M^2\right) \tag{1}$$

M is the molar mass (g mol^{-1}), $\mathrm{d}\Sigma(0)/\mathrm{d}\Omega$ (cm^{-1}) is the scattering intensity at q equal 0, c (g cm^{-3}) is the protein concentration, N_A is Avogadro's number (mol^{-1}), and $\Delta\rho_M$ (cm g^{-1}) is the scattering length density difference per mass.

$$\Delta\rho_M = \Delta\rho\bar{v} \tag{2}$$

The scattering length density difference $\Delta\rho$ (cm^{-2}) can be calculated from the known chemical composition of the protein and the solvent. $\bar{v}$ ($\text{cm}^3\ \text{g}^{-1}$) is the specific volume of the protein in solution, which can be determined via density measurement of the solvent and the solution (DSA 5000; Anton Paar, Graz, Austria).

The aggregation number can be extracted from the ratio between the molar masses of the aggregates and the βlg monomer. The error in the determination of the average molar mass and the aggregation number strongly depends on the data set and is much larger for those where extrapolation to $q = 0$ is difficult to make. Moreover, due to the intricate concentration determination of the different fractions, the actual uncertainty of the values for heat-treated samples is further strongly increased. We estimate the error for the native βlg samples to approximately ±10%, while it is at least ±20% for the heat-treated samples.

2.5. Dynamic and static light scattering

Light scattering experiments were performed using a home-built multi-angle instrument (Moitzi, Vavrin, Bhat, Stradner, & Schurtenberger, 2009) which fully implements the 3D-cross-correlation scheme (Phillies, 1981; Schatzel, 1991; Urban & Schurtenberger, 1998, 1999). It allows for time resolved measurements at 4 angles simultaneously. The 3D-cross-correlation technique suppresses multiply scattered light and provides the scattered intensities and correlation functions that originate from singly scattered light only. A detailed description of the instrument used is given elsewhere (Moitzi et al., 2009).

The native samples and the "soluble" fraction after centrifugation, which are transparent, were measured without dilution. After assuring the integrity of the Mβlg with a concentration series using the 3D-DLS instrument, where their size was shown to be concentration independent, the samples containing Mβlg were diluted 100 fold in MilliQ water prior to the DLS measurements. The size of the particles and their polydispersity was determined in terms of the hydrodynamic radius, which was calculated from the correlation function measured at 120° using the method of cumulants (Koppel, 1972).

3. Results and discussion

3.1. Characterization of unheated β-lactoglobulin solutions

The pH of the native and unheated βlg solution was adjusted between 7.0 and 2.0. All solutions were transparent except the sample at pH 5.6, which was slightly turbid in agreement with previous observations (Mehalebi et al., 2008). A summary of the radius of gyration (R_G), aggregate molar mass (M), and aggregation number (AN) determined by SAXS as well as the hydrodynamic radius (R_H) determined from dynamic light scattering is given in Table 1.

Analysis of the SAXS data reveals the extent of aggregation of unheated βlg increases as the pH approaches the isoelectric point of

Table 1
Summary of the results obtained from SAXS and DLS done at 25 °C on native, unheated βlg solutions (1 wt%) at different pH values. Aggregate molar masses M and aggregation numbers AN were determined using the densities of the sample (e.g. pH 7: 1.000113 g ml^{-1}) and the solvent (0.997290 g ml^{-1}) and applying equations (1) and (2).

pH	R_H (DLS at 120°) [nm]	R_G (SAXS) [nm]	M (SAXS) [g mol^{-1}]	AN (SAXS)
7.0	3.2	2.3	29,000	1.6
6.2	n.d.	2.5	36,000	2.0
5.9	6.5	3.3	49,000	2.7
5.6	n.d.	3.5	59,000	3.2
2.0	3.7	2.1	21,000	1.1

βlg (pH 5.2 for dimers, pH 4.6 for monomers (Hambling et al., 1992; McKenzie, 1971)). This can also be seen in the increase of R_H, which is very sensitive to larger aggregates, when approaching the isoelectric point. In SAXS larger aggregation numbers are indicated by larger plateau heights at low scattering vectors in Fig. 1. The changes with pH can be attributed to the pH dependent charge of the protein. Further away from the isoelectric point larger electrostatic repulsions result in a reduced aggregation number (Aymard, Durand, & Nicolai, 1996; Baussay, Le Bon, Nicolai, Durand, & Busnel, 2004). It has to be noted that the relative error of the SAXS measurements at small scattering angles is less than 3%. Even though the absolute calibration of the scattered intensities and thus the determination of the absolute mass of the aggregates are connected with an error of about 10%, relative changes of a few percent can be seen accurately.

At pH 7 it was necessary to add 5 mM NaCl to screen electrostatic repulsions and avoid interaction effects. Details can be found in chapter 1 in the Supporting information (Figs. S1 and S2).

At pH 2 the plateau at low q-vectors is at significantly lower intensity than for samples at higher pH. Extrapolating the q-vector to zero angle and applying equation (1) gives an aggregation number of 1.1 indicating that βlg is primarily present in monomeric form. This is in agreement with results published by other authors (Aymard et al., 1999). At pH 7.0, the molar mass of the particles is approx. 29,000 g mol^{-1}, which corresponds to a mean aggregation number of 1.6. This is consistent with the fact that mainly dimers are present at this pH (Timasheff et al., 1966). Lowering the pH 7.0 to 6.2, 5.9, and 5.6 respectively constantly increases the mean aggregation number from 1.6 to 3.2. Simultaneously, the radius of gyration increases from 2.3 nm at pH 7.0 to 3.5 nm at pH 5.6. These values are in general higher than reported by Mehalebi et al. (2008), who centrifuged and filtered samples prior to investigation.

When comparing the results obtained from DLS (the hydrodynamic radius) with those obtained from SAXS (the radius of gyration) (see Table 1), the ratio R_G/R_H is surprisingly small for a globular protein, especially at pH values below 7. In our opinion this is due to impurities of relatively large size. These impurities can for instance be aggregates formed by denatured protein. The main reason for the fact that this shows in the ratio R_G/R_H comes from the different q-range used in DLS and SAXS. Large particles contribute mainly at low q, where the DLS experiments have been performed. At the q-values seen by SAXS, the contribution from the large particles has been strongly reduced, and the data used to determine R_G thus contains contributions mostly from monomers/dimers. This is also consistent with the observation that the discrepancy becomes larger when the isoelectric point is approached. At pH 7.0 ($R_G/R_H = 0.72$) the ratio is close to the theoretical value for a homogeneous sphere ($R_G/R_H = 0.77$). Close to the IEP (pH 5.9) we get only $R_G/R_H = 0.51$. Therefore we believe that at pH 7.0 the solution is almost monodisperse (dimers), whereas upon approaching the IEP a small number of larger aggregates form.

The size distributions of the particles are calculated from the SAXS data using the IFT method assuming that all particles are homogeneous, spherical and have the same density (Glatter, 1980). Thus, the calculation is not taking into account the non-spherical shape of dimers and oligomers. This simplifying assumption is necessary because it is not possible to independently determine the size distribution and the shape from a SAXS curve. The results are shown in Fig. 2. At pH 2.0, 98 vol% of βlg particles exhibit a radius of approx. 2.0 nm which can be attributed to individual βlg molecules (Aymard et al., 1999; Griffin, Griffin, Martin, & Price, 1993). The remaining 2% of particles are only slightly larger in radius. At higher pH, the size distributions indicate two or three populations with the most prominent population being slightly larger than 2 nm. At pH 7.0, the primary population is about 2.3 nm in radius (87 vol%), coexisting with a fraction of larger particles (approx. 4 nm, 13 vol%). This result is consistent with the results of Barteri, Gaudiano, Rotella, Benagiano, and Pala (2000) who described βlgA at pH 7.0 as monodisperse dimers with a R_G of 2.1 nm (in 20 mM Tris buffer at 0.002−0.004%). Other authors also reported that at this pH mainly dimers are present, although it was mentioned that higher aggregates can be found in solution but were discarded from the analysis (Panick, Malessa, & Winter, 1999) or that the polydispersity index suggests that small amounts of low molecular weight aggregates may occur (pH 7.8, 0.05 M phosphate buffer). At higher protein concentration (8 wt%) the presence of aggregates with a hydrodynamic radius of 100 nm at pH 7.0 was reported (imidazole buffer 10 mM) (Haque & Sharma, 1997). In order to explain the differences observed within literature, the influence of sample preparation and the source of the protein powder should be further investigated. Indeed the source of βlg and the method of sample preparation may have a great impact on the formation of

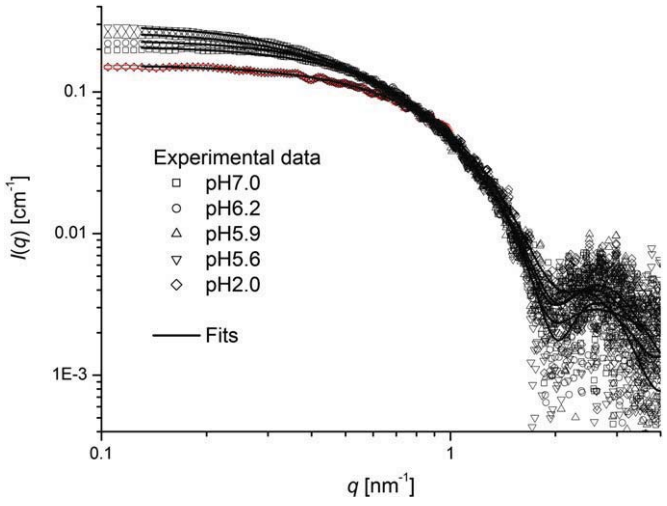

Fig. 1. SAXS curves of unheated 1 wt% β-lactoglobulin at 25 °C adjusted to different pH values and corresponding fits from the indirect Fourier transformation. Data are slit smeared. For the data measured at pH 2 also the error bars are shown to illustrate that the relative changes of the scattered intensities with pH are highly significant.

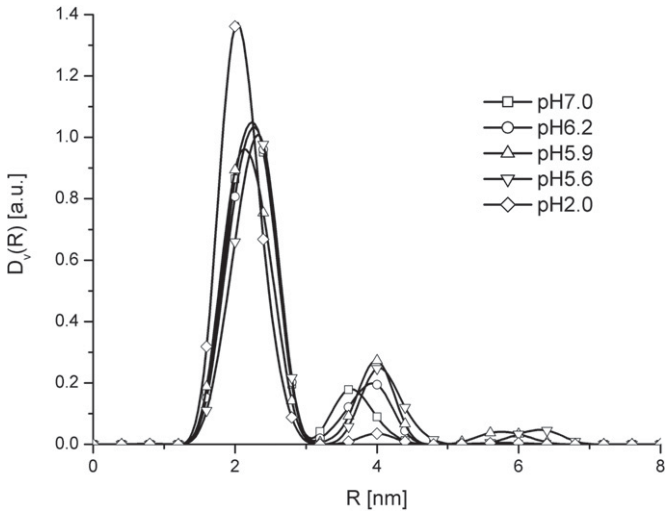

Fig. 2. Volume weighted size distributions of 1% βlg at 25 °C as a function of pH calculated from the SAXS curves assuming homogeneous spherical particles. The area under the curves was normalized to 1.

aggregates (Cromwell, Hilario, & Jacobson, 2006). In the study at hand βlg was freeze dried at a pH close to the isoelectric point of βlg monomers (pH 4.6), which might increase the average particle sizes and explain the oligomers observed by SAXS.

Adjusting the pH from 7.0 towards the isoelectric point does not change the main peak in the size distribution function (Fig. 2) but rather increases the fraction of the aggregates with a radius of ~4 nm. This population increases from 13 vol% at pH 7.0 to 15 vol% at pH 6.2 and reaches 21–22 vol% at pH 5.9 and pH 5.6. At pH 5.6 and 5.9, a third population (4 vol%) with a radius of ~6 nm is visible. This is consistent with the changes in R_G and R_H reported in Table 1.

The composition of these larger aggregates and the mechanism driving the formation of these particles is still a matter of debate. Also previous work was showing larger particle fractions in the pH range from 5.6 to 5.9 (Donato et al., 2009; Schmitt et al., 2009). Presumably, reduced electrostatic repulsion favors the formation of equilibrium aggregates when the pH is lowered.

3.2. Characterization of β-lactoglobulin solution heated at pH 5.9

The solutions of β-lactoglobulin at pH 5.9 (1 wt%) were heated in a water bath. Without heating, the solutions are stable (they do not precipitate) at this pH for a long time (see Supporting information Fig. S3).

3.2.1. Evolution of the soluble and insoluble protein fractions with heating time

The composition of the heated samples is shown in Fig. 3 as a function of the heating protocol. Increasing the temperature increases the amount of the insoluble fraction (Mβlg) and deprives the solution of native protein. Heating the βlg solution at 85 °C for 15 min results in approximately 70% insoluble aggregates and the pH shifts from 5.9 to 6.45. Longer heating times have only a minor effect on the insoluble fraction (Mβlg), but increase the amount of soluble aggregates up to 18% and the pH to about 6.6 after 8 h. We can thus speculate that upon heating, unfolded βlg first aggregates and forms Mβlg until a holding time of 15 min at 85 °C. At longer heating times the shift in the pH of the sample results in the formation of smaller soluble aggregates because of increased electrostatic repulsion and change in the aggregation mechanism (Donato et al., 2009).

3.2.2. Experimental approach for structural characterization of the insoluble and soluble βlg fractions formed upon heating

In order to get insight into the structure of the different aggregates present in the heated samples, the small-angle X-ray scattering data of the insoluble (Mβlg) and soluble fractions (soluble aggregates and residual native protein) were analyzed separately applying the following procedure.

The SAXS signal of the Mβlg fraction was deduced from the difference between the scattering signal of the whole heated sample and the scattering signal of the supernatant after centrifugation. By subtracting the scattering signal of water from the scattering signal of the supernatant, the scattering curve of the soluble fraction was obtained. The SAXS curves before and after subtraction are shown in Fig. 4 A and B.

3.2.3. Structural analysis of the insoluble fraction containing Mβlg

The combined scattering curves from SAXS and light scattering of Mβlg obtained at various stages of the heating protocol are shown in Fig. 5A. The *q*-regime of the SAXS measurements was extended by the static light scattering data down to a value of 0.0027 nm^{-1}. The corresponding structural features are summarized in Table 2. Samples heated to 60 °C were not measurable since a small precipitate was found after cooling, indicating large aggregates which were not further analyzed. Heating samples further up to 85 °C resulted in Mβlg with R_H around 130 nm. The determined radii compare well with R_H ~ 120 nm reported in literature (Donato et al., 2009; Jung et al., 2008; Schmitt et al., 2009) after heating 1 wt% βlg solutions at pH 5.8–5.9 for 15 min at 85 °C. However, Mehalebi et al. (2008) reported a R_H of 20 nm, after heating a 1 wt% βlg solution at pH 6.0 for 15 h at 80 °C. The difference can be tentatively explained by the sensitivity of the system, with subtle changes in pH or centrifugation and filtration procedures greatly impacting the size of the aggregates. The apparent molar mass of Mβlg was determined from SAXS measurements and their aggregation number was deduced. At 70 °C the aggregation number is about 30,000 and stays practically constant up to 75 °C. Thereafter, the mean aggregation number increases to a maximum of 50,000 after 15 min at 85 °C. The

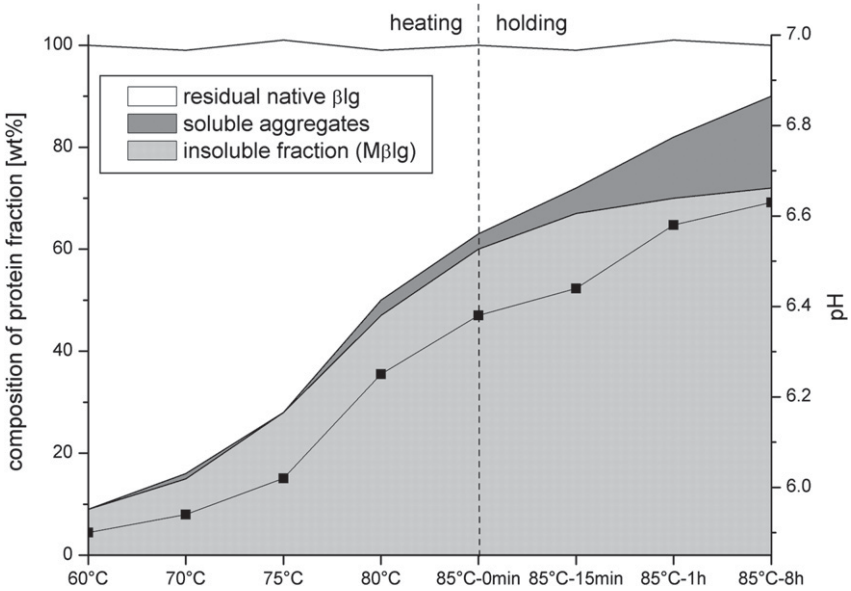

Fig. 3. Composition and pH (symbols) of the 1 wt% βlg solution (initial pH = 5.9) during the heating up to 85 °C and subsequent holding time.

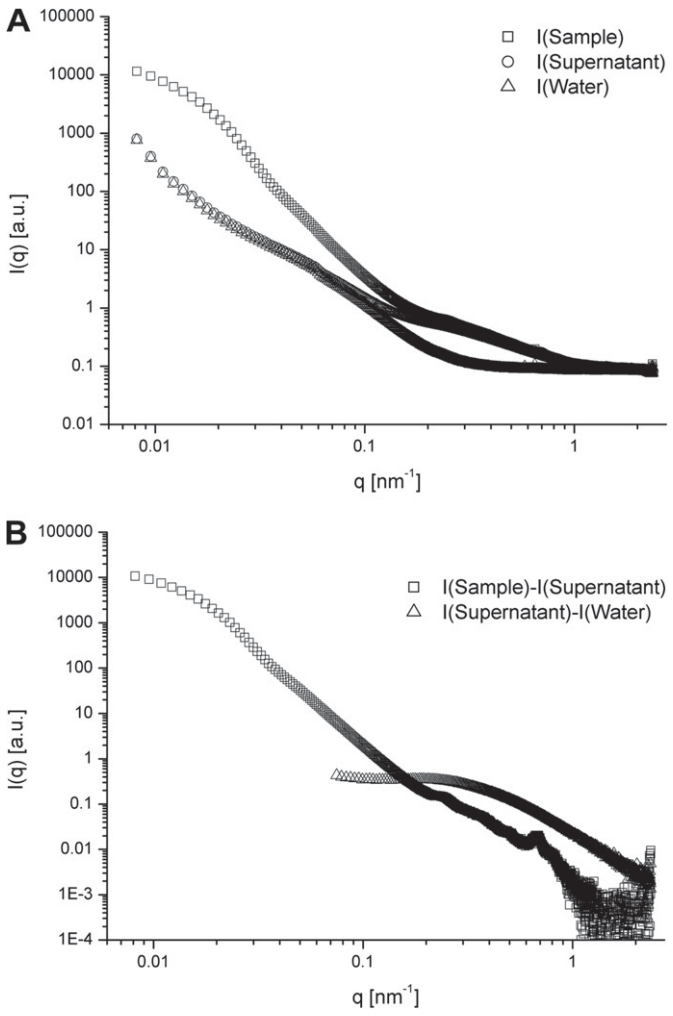

Fig. 4. A. Raw SAXS curves of a heated 1 wt% βlg solution (85 °C, 0 min), the supernatant after centrifugation and water. **B**. Scattering curves of the insoluble fraction (I(sample) − I(supernatant)) containing Mβlg and the soluble fraction (I(supernatant) − I(water)) containing soluble aggregates and residual native βlg.

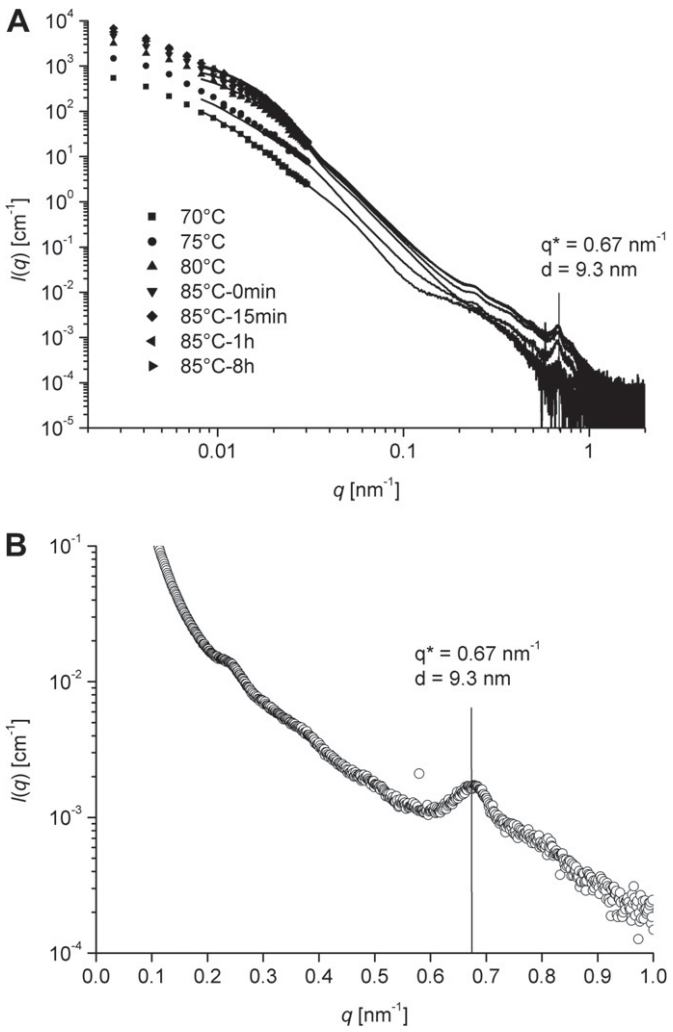

Fig. 5. A. Scattering curves of the insoluble fraction (calculated as shown in Fig. 4) measured as a function of the heating protocol. The q-regime of the SAXS measurements (lines) is significantly extended by the static light scattering data (symbols). The light scattering intensities were scaled to overlap with the SAXS data. The same scaling factor was used for all shown curves. **B**. Close-up of the peak which appears in the SAXS pattern of Mβlg at the end of the heating procedure.

corresponding M is 9.2×10^8 g mol^{-1}, which is twice the value reported at pH 5.8 by Jung et al. (2008). However, in our determination the signal of the soluble fraction (approx. 30% of the protein) was subtracted from the scattering curve. Therefore, the determination of the mean molar mass of the Mβlg is not distorted by soluble aggregates and residual native protein. After 8 h of heating, the observed aggregation number decreases again down to 30,000. The fluctuation of the average aggregation number during these 8 h most probably reflects the experimental error mainly resulting from the extrapolation of the SAXS data to $q = 0$ and the uncertainties in the concentration determination. However, we might also speculate that the trend of a decreasing average molar mass after long heating times may partially be due to the formation of new particles with relatively low molar mass, but yet large enough to settle during the centrifugation step. The formation of these relatively small particles, which is also reflected in the strongly increasing amount of soluble aggregates as the time of heating proceeds (see Fig. 3) might be driven by the increasing charge of the proteins due to the increasing pH. However, due to the fact that at 85 °C almost all of the microgels have already been formed, it is also obvious that the formation of some additional smaller aggregates can not be sufficient to explain the relatively large variations in the average aggregation number.

The radius of gyration R_G was determined by the IFT algorithm. This was complicated by the fact that the scattering curves of the heated samples showed an upturn at small scattering angles. This behavior is typical for larger particles present in the sample and an indication of polydispersity. Given the difficulties to analyze scattering data from polydisperse samples it was necessary to fractionate the sample in order to get a narrow monomodal particle distribution. Therefore, the 85 °C 15 min sample was subjected to varying centrifugation cycles to remove the largest particles. After gentle centrifugation for 6 h at 450 g a very long linear regime in

Table 2
Summary of the calculated structural features obtained from SAXS and light scattering for the Mβlg fraction obtained during heating to 85 °C.

Temp. [°C]	Time [min]	R_H (DLS at 120°) [nm]	R_G (SAXS) [nm]	Conc. Mβlg [wt%]	M (SAXS) [$\times 10^8$ g mol^{-1}]	AN (SAXS)
70	0	156	133	0.154	5.27	29,000
75	0	114	125	0.284	5.03	27,000
80	0	120	118	0.472	6.56	36,000
85	0	126	119	0.598	7.18	39,000
85	15	138	121	0.675	9.20	50,000
85	60	141	120	0.697	8.49	46,000
85	480	150	118	0.722	5.46	30,000

the Guinier plot was observed (see Supporting information Fig. S4). Also the angular dependence of R_H is becoming weaker after the centrifugation procedure (see Supporting information Fig. S5). The R_G after centrifugation for 6 h was 54 nm and R_H was 90 nm. Now the precondition of a relatively narrow monomodal distribution is fulfilled, which allows for a more detailed characterization of the internal structure of the particles. Homogeneous spheres are characterized by a value for $R_G/R_H = 0.775$ (Burchard, 1994). Here we now measured $R_G/R_H = 0.6$, which is slightly higher than the value of 0.56 found by Jung et al. (2008) after heating 1 wt% βlg at pH 5.8. Nevertheless, both values are significantly smaller than 0.775, which is characteristic for particles with a denser core and a less dense outer shell. In literature values of approx. $R_G/R_H = 0.6$ are typically found for microgel particles (Senff & Richtering, 1999).

The SAXS curves of the insoluble fraction, shown in Fig. 5A, feature a characteristic peak. A close-up is shown in Fig. 5B. The position of the peak ($q^* = 0.67\ nm^{-1}$) corresponds to a typical distance d of 9.3 nm ($d = 2p/q^*$) in real space. The length scale of this structural correlation is larger than the size of the primary building units (dimers of approx. 6 nm). We may speculate that Mβlg are build up by oligomers that form as a transient state during the heating procedure. It is interesting to note that the typical distance of about 9 nm roughly corresponds to the size of the larger aggregates found before heating (hydrodynamic diameter of about 8 nm; see Fig. 2). However, the role of these larger aggregates in the mechanism of Mβlg formation remains unclear and no explicit relation can be drawn from the present structural analysis. A similar multiscale structure has recently been described in covalent whey protein microgels (Schmitt et al., 2010).

3.2.4. Structural analysis of the soluble protein fraction

Most of the scattering curves of the supernatants collected from the heated samples are very similar in shape to the scattering curve of native protein. Only the supernatant of the sample which was heated for 8 h at 85 °C shows a different profile. In Fig. 6 the concentration normalized SAXS curves of the soluble fraction at different stages of the heating protocol are shown. Differences in the height of those SAXS curves that mainly contain native protein can to a large extend be attributed to the error in the protein concentration determination.

At the beginning of the heat treatment the soluble fraction is mainly composed of native proteins, and the scattering signal is dominated by them. The mean aggregation number is around 3 up to a holding time of 1 h at 85 °C (Table 3). The respective values for R_G are around 2.5 nm. Considering the uncertainties in the sample preparation and the instrumental technique these values compare well with those obtained with the unheated sample (Table 1). Thus SAXS measurements can provide us with an at least rough characterization of the low molecular weight fraction present in the supernatant as long as the fraction of the soluble aggregates is not dominating. When looking at Fig. 3 it is obvious that the overall amount of soluble aggregates already increases strongly as soon as the sample is heated to 85 °C. However, the intensity scattered by a mixture of two populations seen at the q-range of the SAXS experiment depends on the relative concentrations, the masses and the form factors. Up to 1 h the contribution from the much larger soluble aggregates is thus still masked by the native proteins, and only when the concentration ratio between the soluble aggregates and the native proteins increases enough, this can then compensate for the much smaller form factor of the soluble aggregates in the accessible q-range. This happens at 85 °C after longer heating times, where the presence of an increased relative amount of comparably large, soluble aggregates makes a determination of R_G of the low molecular weight fraction impossible.

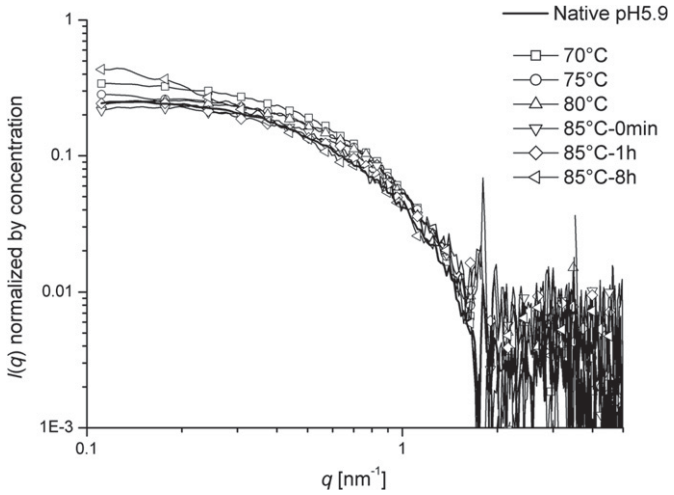

Fig. 6. Small-angle X-ray scattering curves of the soluble fraction (I(supernatant) − I(water)) of 1 wt% βlg samples at different stages of the heating protocol. The scattering curve of the unheated native protein at pH 5.9 is shown as well. All data were put on absolute scale and normalized by the protein concentration. The data are slit smeared.

Table 3
Summary of the results of SAXS and light scattering of the soluble fraction (soluble aggregates and native protein) obtained at different stages of the heating protocol.

Temp. [°C]	Time [min]	R_H (DLS at 120°) [nm]	R_G (SAXS) [nm]	Conc. [wt%]	M (SAXS) [g mol^{-1}]	AN (SAXS)
70	0	55	2.3	0.833	65,000	3.5
75	0	62	2.9	0.726	58,000	3.2
80	0	31	2.5	0.529	58,000	3.2
85	0	43	2.1	0.402	42,000	2.3
85	60	29	2.8	0.325	51,000	2.8
85	480	26	n.d.	0.279	n.d.	n.d.

Contrariwise, dynamic light scattering is sensitive to the other fraction of the supernatant. Here it is the large soluble aggregates, which completely dominate the scattering signal. This is already the case at the beginning of the heating procedure, at 70 °C, although there the weight fraction of the soluble aggregates is almost vanishing compared to the residual native βlg. At 85 °C the fraction of soluble aggregates just starts to become significant and constitutes a few weight percent of the total protein amount of the original βlg solution (see Fig. 3). This fraction further increases with increasing heating time. At this point it is important to recall the fact that the differentiation between "soluble aggregates" and "insoluble aggregates" is based on our deliberately chosen centrifugation procedure (see Figs. S4 and S5 in Supporting information). It is thus a broad distribution of aggregates rather than two distinct populations, which can easily be separated that we have to deal with.

Combining the information obtained from SAXS and DLS we can conclude that neither the size nor the mass of the particles present in the soluble fraction change significantly during the heating procedure. What changes is the relative amount of soluble aggregates (with R_H around 30–60 nm as determined from DLS) compared to native protein (with R_G around 2.5 nm, as determined from SAXS).

We think that the increasing pH of the samples (Fig. 3) is favoring the formation of rather small aggregates (also showing up in the soluble fraction) as compared to Mβlg, which forms at the beginning of the heat treatment and whose amount does not increase considerably any more during the prolonged heating at 85 °C.

4. Conclusion

This study follows the formation of βlg microgels (Mβlg) upon heating a 1 wt% βlg solution up to 85 °C with X-ray and light

scattering experiments on selected stages during a defined heating protocol. Upon heating the protein solution at pH 5.9, Mβlg – or so-called "insoluble aggregates" – with a hydrodynamic radius of approximately 130 ± 20 nm start to form as temperature increases above 60 °C. After 15 min at 85 °C, about 70% of the protein is transformed to Mβlg. SAXS measurements on absolute scale provide us with average aggregation numbers of around 40,000 for these microgels. The internal mass distribution of Mβlg is not homogeneous but rather concentrated in the center of the particle ($R_G/R_H = 0.6$; determined after 15 min at 85 °C), which very much resembles the results found for synthetic microgel particles (Senff & Richtering, 1999).

During prolonged heating of the sample at 85 °C, the process continues, but now the remaining native protein mainly forms relatively small so-called "soluble aggregates", most likely because of the pH increase due to protein denaturation (pH at 70 °C ~ 6.0; pH after 8 h at 85 °C ~ 6.6).

In the first stages of the heating procedure the soluble fraction is mainly composed of residual native proteins, while soluble aggregates start to form at around 85 °C and make up almost 2/3 of the soluble fraction at the end of the heating procedure, i.e. after 8 h at 85 °C. At the same time the amount of Mβlg increases only marginally during the holding time at 85 °C.

It is interesting to mention that the SAXS curves of Mβlg exhibit a correlation peak corresponding to a characteristic distance of 9.3 nm indicating a structural organization within the microgels (Schmitt et al., 2010).

In the future it would be interesting to investigate the effect of the complex interplay between temperature, protein concentration and protein source and composition on the resulting Mβlg in order to further elucidate their formation mechanism.

Acknowledgements

This work was co-financed by the Nestlé Research Center, Lausanne, Switzerland, the University of Fribourg, Switzerland, and the Adolphe Merkle Foundation. The SAXS experiments were partially done at the X12SA (cSAXS) beamline at the Swiss Light Source, Paul Scherrer Institute, Villigen, Switzerland. We thank our local contact Dr. Andreas Menzel. Dr. Martin Leser from Nestlé Research Center is thanked for his input during scientific discussions. Miss Céline Jordan from the Nestlé Research Center is thanked for technical support during the gel electrophoresis preparation.

Appendix. Supporting information

Supplementary data associated with this article can be found, in the online version

References

Aymard, P., Durand, D., & Nicolai, T. (1996). The effect of temperature and ionic strength on the dimerisation of beta-lactoglobulin. *International Journal of Biological Macromolecules, 19*(3), 213–221.

Aymard, P., Nicolai, T., Durand, D., & Clark, A. (1999). Static and dynamic scattering of beta-lactoglobulin aggregates formed after heat-induced denaturation at pH 2. *Macromolecules, 32*(8), 2542–2552.

Barteri, M., Gaudiano, M. C., Rotella, S., Benagiano, G., & Pala, A. (2000). Effect of pH on the structure and aggregation of human glycodelin A. A comparison with beta-lactoglobulin A. *Biochimica et Biophysica Acta – Protein Structure and Molecular Enzymology, 1479*(1–2), 255–264.

Baussay, K., Le Bon, C., Nicolai, T., Durand, D., & Busnel, J. P. (2004). Influence of ionic strength on the heat-induced aggregation of the globular protein beta-lactoglobulin at pH 7. *International Journal of Biological Macromolecules, 34*(1–2), 21–28.

Bergmann, A., Orthaber, D., Scherf, G., & Glatter, O. (2000). Improvement of SAXS measurements on Kratky slit systems by Göbel mirrors and imaging-plate detectors. *Journal of Applied Crystallography, 33*, 869–875.

Bromley, E. H. C., Krebs, M. R. H., & Donald, A. M. (2006). Mechanisms of structure formation in particulate gels of β-lactoglobulin formed near the isoelectric point. *The European Physical Journal E, 21*, 145–152.

Bryant, C. M., & McClements, D. J. (1998). Molecular basis of protein functionality with special consideration of cold-set gels derived from heat-denatured whey. *Trends in Food Science & Technology, 9*(4), 143–151.

Burchard, W. (1994). *Light scattering*. Glasgow: Blackie Academic and Professional.

Casal, H. L., Kohler, U., & Mantsch, H. H. (1988). Structural and conformational-changes of beta-lactoglobulin-B – an infrared spectroscopic study of the effect of pH and temperature. *Biochimica et Biophysica Acta, 957*(1), 11–20.

Cromwell, M. E. M., Hilario, E., & Jacobson, F. (2006). Protein aggregation and bioprocessing. *AAPS Journal, 8*(3), E572–E579.

de Wit, J. N. (1998). Nutritional and functional characteristics of whey proteins in food products. *Journal of Dairy Science, 81*, 597–608.

Donald, A. M. (2008). Aggregation in beta-lactoglobulin. *Soft Matter, 4*, 1147–1150.

Donato, L., Schmitt, C., Bovetto, L., & Rouvet, M. (2009). Mechanism of formation of stable heat-induced beta-lactoglobulin microgels. *International Dairy Journal, 19*(5), 295–306.

Gimel, J. C., Durand, D., & Nicolai, T. (1994). Structure and distribution of aggregates formed after heat-induced denaturation of globular proteins. *Macromolecules, 27*, 583–589.

Glatter, O. (1977). A new method for the evaluation of small-angle scattering data. *Journal of Applied Crystallography, 10*, 415–421.

Glatter, O. (1980). Determination of particle-size distribution functions from small-angle scattering data by means of the indirect transformation method. *Journal of Applied Crystallography, 13*, 7–11.

Griffin, W. G., Griffin, M. C. A., Martin, S. R., & Price, J. (1993). Molecular basis of thermal aggregation of bovine beta-lactoglobulin A. *Journal of Chemical Society – Faraday Transactions, 89*(18), 3395–3406.

Guinier, A., & Fournet, G. (1955). *Small angle scattering of X-rays*. New York: Wiley.

Hambling, S. G., McAlpine, A. S., & Sawyer, L. (1992). *Advanced dairy chemistry*. London: Elsevier Science Publishers Ltd.

Haque, Z. U., & Sharma, M. (1997). Thermal gelation of beta-lactoglobulin AB purified from Cheddar whey. I. Effect of pH on association as observed by dynamic light scattering. *Journal of Agricultural and Food Chemistry, 45*, 2958–2963.

Jung, J. M., Savin, G., Pouzot, M., Schmitt, C., & Mezzenga, R. (2008). Structure of heat-induced beta-lactoglobulin aggregates and their complexes with sodium-dodecyl sulfate. *Biomacromolecules, 9*(9), 2477–2486.

Kavanagh, G. M., Clark, A. H., & Ross-Murphyand, S. B. (2000). Heat-induced gelation of globular proteins: part 3. Molecular studies on low pH -lactoglobulin gels. *International Journal of Biological Macromolecules, 8*, 41–50.

Koppel, D. E. (1972). Analysis of macromolecular polydispersity in intensity correlation spectroscopy: the method of cumulants. *Journal of Chemical Physics, 57*, 4814–4820.

Kratky, O., Porod, G., & Kahovec, L. (1951). Some innovations in the technique and evaluation of X-ray small-angle measurements. *Zeitschrift fuer Elektrochemie und Angewandte Physikalische Chemie, 55*, 53–59.

Langton, M., & Hermansson, A. M. (1992). Fine-stranded and particulate gels of beta-lactoglobulin and whey-protein at varying pH. *Food Hydrocolloids, 5*(6), 523–539.

Lindner, P., & Zemb, T. (2002). *Neutrons, X-rays and light: Scattering methods applied to soft condensed matter*. Amsterdam: Elsevier Science.

McKenzie, H. A. (1971)*Milk proteins chemistry and molecular biology, Vol. 2*. London: Academic Press.

Mehalebi, S., Nicolai, T., & Durand, D. (2008). Light scattering study of heat-denatured globular protein aggregates. *International Journal of Biological Macromolecules, 43*(2), 129–135.

Moitzi, C., Vavrin, R., Bhat, S. K., Stradner, A., & Schurtenberger, P. (2009). A new instrument for time-resolved static and dynamic light-scattering experiments in turbid media. *Journal of Colloid and Interface Science, 336*, 565–574.

Morr, C. V., & Ha, E. Y. W. (1993). Whey-protein concentrates and isolates – processing and functional-properties. *Critical Reviews in Food Science and Nutrition, 33*(6), 431–476.

Mulvihill, D. M., & Donovan, M. (1987). Whey proteins and their thermal denaturation – a review. *Irish Journal of Food Science and Technology, 11*, 43–75.

Orthaber, D., Bergmann, A., & Glatter, O. (2000). SAXS experiments on absolute scale with Kratky systems using water as a secondary standard. *Journal of Applied Crystallography, 33*, 218–225.

Panick, G., Malessa, R., & Winter, R. (1999). Differences between the pressure- and temperature-induced denaturation and aggregation of beta-lactoglobulin A, B, and AB monitored by FT-IR spectroscopy and small-angle X-ray scattering. *Biochemistry, 38*(20), 6512–6519.

Phillies, G. D. J. (1981). Experimental demonstration of multiple-scattering suppression in quasielastic-light-scattering spectroscopy by homodyne coincidence techniques. *Physical Review A, 24*(4), 1939–1943.

Schatzel, K. (1991). Suppression of multiple-scattering by photon cross-correlation techniques. *Journal of Modern Optics, 38*(9), 1849–1865.

Schmitt, C., Bovay, C., Vuilliomenet, A. M., Rouvet, M., Bovetto, L., Barbar, R., et al. (2009). Multiscale characterization of individualized beta-lactoglobulin microgels formed upon heat treatment under narrow pH range conditions. *Langmuir, 25*(14), 7899–7909.

Schmitt, C., Moitzi, C., Bovay, C., Rouvet, M., Bovetto, L., Donato, L., et al. (2010). Internal structure and colloidal behaviour of covalent whey protein microgels obtained by heat treatment. *Soft Matter, 6*, 4876–4884.

Senff, H., & Richtering, W. (1999). Temperature sensitive microgel suspensions: colloidal phase behavior and rheology of soft spheres. *Journal of Chemical Physics, 111*(4), 1705–1711.

Timasheff, S. N., Mescanti, L., Basch, J. J., & Townend, R. (1966). Conformational transitions of bovine beta-lactoglobulins A, B and C. *Journal of Biological Chemistry, 241*(11), 2496–2501.

Urban, C., & Schurtenberger, P. (1998). Characterization of turbid colloidal suspensions using light scattering techniques combined with cross-correlation methods. *Journal of Colloid and Interface Science, 207*, 150–158.

Urban, C., & Schurtenberger, P. (1999). Application of a new light scattering technique to avoid the influence of dilution in light scattering experiments with milk. *Physical Chemistry Chemical Physics, 1*, 3911–3915.